Research Square

Preprints are preliminary reports that have not undergone peer review.
They should not be considered conclusive, used to inform clinical practice,
or referenced by the media as validated information.

Strigolactone analog GR24 modulates hyphal growth, mitochondrial activity, and superoxide accumulation in the ectomycorrhizal fungus Rhizopogon roseolus

Mutiara Nur Pratiwi
Tottori University
Kaeoniwong Nathawan
Tottori University
Somboon Chollada
Tottori University
Azakami Hiroyuki
Yamaguchi University
Tadanori Aimi
Tottori University
Norihiro Shimomura
nshimo@tottori-u.ac.jp

Tottori University

Research Article

Keywords: Branching factor, Mycorrhiza, Presymbiotic signaling, Reactive oxygen species

Posted Date: November 3rd, 2026

DOI: https://doi.org/10.21203/rs.3.rs-11408684/v1

License: This work is licensed under a Creative Commons Attribution 4.0 International License.
Read Full License

Additional Declarations: No competing interests reported.

Abstract

Plant hormone strigolactone (SL) is an important rhizosphere signal that mediate communication between plants and diverse soil organisms. However, the role of SL in ectomycorrhizal (ECM) fungi remains largely unexplored, despite ECM fungi representing a major group of plant symbiotic fungi. To address this knowledge gap, we examined the effects of widely used SL analog GR24 with different stereoisomers and concentrations on several ECM fungal species. Deeper investigation on cellular and transcriptional response to GR24 was conducted on *Rhizopogon roseolus*. The evaluated parameters include fungal growth and branching, mitochondrial activity, superoxide accumulation, Ca^{2+} signaling, and gene expression. Our findings reveal that ECM fungal responses to GR24 depend on fungal species, as well as GR24 stereoisomers and concentration. Further analysis on *R. roseolus* suggested that GR24 enhanced mitochondrial activity and increased mitochondria-associated superoxide accumulation. Based on pharmacological approach, the response of *R. roseolus* to GR24 required extracellular Ca^{2+} influx. Consistent with these morphological and cellular responses, GR24 induce transcriptional response in genes related to cell-wall biosynthesis, mitochondrial respiratory chain, superoxide detoxification, and Ca^{2+} signaling. Together, these findings provide novel insight into SL responsiveness in ECM fungi by integrating morphological, cellular, and transcriptional analyses.

Introduction

Strigolactone (SL) is a class of carotenoid-derived compound that function as plant hormone and rhizosphere signal. Notably, the role of SL as rhizosphere signal was recognized long before their role as plant hormones was established. The first isolated SL compound, Strigol, was found in root exudate of cotton plant (*Gossypium hirsutum*) and induced the germination of root-parasitic plant *Striga lutea* (Cook et al. 1966). Another natural SL, 5-deoxystrigol, was isolated from legume *Lotus japonicus* and induced hyphal branching of arbuscular mycorrhizal (AM) fungus *Gigaspora margarita* (Akiyama et al. 2005). SL were later established as plant hormone through their role as endogenous regulators of shoot branching (Gomez-Roldan et al. 2008; Umehara et al. 2008). Since then, investigation on SL biosynthesis, structural diversity, and signaling has been extensively conducted on plants (Hamiaux et al. 2012; Alder et al. 2012; Nakamura et al. 2013; Wang and Bouwmeester 2018). In contrast, the mechanism underlaying SL response in other organisms, especially fungi, remain poorly understood.

SL responses have been reported in various plant-associated fungi, including AM, endophytic, and pathogenic fungi. Across these fungal groups, SL treatment has been associated with changes in redox regulation, including reactive oxygen species (ROS) homeostasis and antioxidant activity (Besserer et al. 2008; Belmondo et al. 2017; Rozpądek et al. 2018). Although SL affect some similar cellular responses among fungal groups, their physiological outcomes may depend on fungal ecological lifestyles. SL inhibited the growth of endophytic and pathogenic fungi, with their effects on hyphal branching vary across species (Dor et al. 2011; Rozpądek et al. 2018). Coherently, previous studies reported that SL contributed to plant resistance against pathogenic fungi (Torres-Vera et al. 2014; Decker et al. 2017; Vogel et al. 2023; Fujita et al. 2024). On the other hand, SL promoted development of AM fungi by

stimulating spore germination, increasing hyphal branching, inducing mitochondrial activity, and promoting root colonization (Akiyama et al. 2005; Besserer et al. 2008; Gomez-Roldan et al. 2008). SL also induced AM fungus to produce and secrete signals required for colonization (Genre et al. 2013; Tsuzuki et al. 2016).

Compared with other plant-associated fungi, the role of SL in ectomycorrhizal (ECM) remains largely unexplored. ECM is a major group of symbiotic fungi that colonize the root of woody plants and facilitate their nutrient uptake. Previous study reported that SL analog GR24 did not affect hyphal branching in ECM fungi *Paxillus involutus*, *Laccaria bicolor*, *Amanita muscaria*, and *Cenococcum geophilum*; although the authors explicitly regarded these observations as preliminary (Steinkellner et al. 2007). Natural SL, 5-deoxystrigol, induced melanin secretion in *Pisolithus tinctorius* without affecting fungal growth (Herrera-Martínez et al. 2014). Garcia et al. (2015) stated that the absence of an obvious growth response did not necessarily exclude a role for SL in ECM. Importantly, SL and its related metabolites have been isolated from root exudates of several ECM host plants, including *Populus tricharpa*, *Pinus thunbergii*, and *P. greggii* (Herrera-Martínez et al. 2014; Xie 2016; Yoneyama et al. 2018). These observations suggest that ECM fungi may encounter SL or related lactones in the rhizosphere of host plants, yet whether they can perceive and respond to these compounds remains largely unresolved.

To address this knowledge gap, we examined the effects of widely used SL analog GR24 at different structures and concentrations on several ECM fungi species and elucidated the underlying response mechanism in *Rhizopogon roseolus* TUFC10010. *R. roseoulus* is an edible ECM fungus associated with *Pinus* spp. and has been studied for artificial cultivation (Shimomura et al. 2012). The TUFC10010 is a superior isolate that has high and rapid ectomycorrhiza-forming ability while still capable of growing independently of its host, making it suitable for investigating direct fungal response under controlled laboratory conditions (Shimomura et al. 2012; Putra et al. 2022). We assessed ECM fungal responses to GR24 by examining fungal growth and branching, mitochondrial activity, ROS accumulation, Ca^{2+} signaling, and gene expression. Our results reveal that ECM fungal responses to GR24 depend on fungal species, as well as GR24 structure and concentration. We propose that GR24 modulates hyphal growth, mitochondrial activity, and superoxide accumulation in the ectomycorrhizal fungus in *Rhizopogon roseolus* TUFC10010. This is the first study to provide detailed information on the cellular and transcriptional response of ECM fungi to SL.

Materials and methods

Fungal material

This study used six ECM fungal isolates, including *R. roseolus* (= *R. rubescens*) TUFC10010, *Suillus granulatus* TUFC31903, *Laccaria bicolor* TUFC101044, *Lyophyllum shimeji* TUFC30169, *Amanita manginiana* TUFC100797, *Russula bella* TUFC101232. Fungal isolates were obtained from the Fungus/Mushroom Resource and Research Center, Faculty of Agriculture, Tottori University, with support from the National BioResource Project of MEXT, Japan (https://nbrp.jp/en/). All fungal isolates were

initially cultured on malt extract agar (MEA) and incubated in the dark at 25°C for 4 weeks. For subsequent experiment, a 5-mm agar plug from each culture was subsequently transferred to 1/5MMN agar medium and incubated under the same condition in 4 weeks.

Chemicals

The strigolactone analog (–)-GR24 (hereafter GR24; Toronto Research Chemicals Inc., Canada) and rac-GR24 (Chiralix, The Netherlands) were dissolved in acetone to prepare 10^{-3} M stock solution and diluted in sterile solvent to final concentrations of 10^{-6} or 10^{-8} M. MitoTracker™ Red CMXRos (Invitrogen, USA) was dissolved in dimethyl sulfoxide (DMSO) to prepare 1 mM stock solution and diluted in phosphate-buffered saline (PBS) to a final concentration of 100 nM. Nitroblue tetrazolium chloride (NBT; Dojindo Laboratories, Japan) was dissolved in 0.1 mM PBS to a final concentration 0.05%. Chloramphenicol (FUJIFILM Wako Pure Chemical Corporation, Japan) was dissolved in 70% ethanol and diluted in 0.1 mM PBS to a final concentration 1 mg/mL. EDTA 0.5 M pH 8.0 (FUJIFILM Wako Pure Chemical Corporation, Japan) diluted in distilled water to a final concentration 0.5 mM. EGTA (Dojindo Laboratories, Japan) diluted in distilled water to final a concentration 1 mM. Verapamil hydrochloride (FUJIFILM Wako Pure Chemical Corporation, Japan) was dissolved in DMSO and diluted in 0.1 mM PBS to 10 µM. RNA extraction, reverse transcription, and qPCR was conducted using TRIzol™ Reagent (Invitrogen, USA), ReverTra Ace® qPCR RT Master MIX with gDNA Remover (TOYOBO, Japan) and KOD SYBR™ qPCR/RT (TOYOBO, Japan).

Hyphal branching analysis

The experiment was conducted on all six ECM fungal isolates. A 5-mm agar plug of each isolate was inoculated onto a glass slide that previously had been coated with a thin layer of 1/5MMN agar and placed on 2% water agar in a Petri dish. Treatment with 10 µL of GR24 or rac-GR24 at 10^{-8} M or 10^{-6} M, diluted in 1/5MMN medium, was applied directly to both sides of the fungal plug. Sterile 1/5MMN liquid medium was used as negative control. The cultures were incubated in the dark at 25°C until the colonies reached approximately 1 cm in diameter. The incubation period was varied across isolates depend on their growth rates. After incubation, fungal colonies were stained with lactophenol cotton blue to improve visualization under a light microscope (Nikon Eclipse 80i, Japan). The number of primary branches was counted within a 1000-µm length from the hyphal tip. Each experimental group consisted of six biological replicates, with 30 hyphae examined per replicate.

Fungal biomass analysis

This experiment was conducted on all six ECM fungal isolates. A 5-mm fungal plug of was inoculated into 25 mL of 1/5MMN liquid medium supplemented with GR24 at a final concentration of 10^{-8} M. Cultures for negative control were inoculated in 1/5MMN liquid medium without GR24 supplementation.

All cultures were incubated in the dark at 25°C for 5 weeks. Each experimental group consisted of six biological replications. After incubation, fungal mycelia were separated from the medium by vacuum filtration and dried in an oven at 60°C for 15 hours. Mycelial dry weight was measured using an analytical balance.

MitoTracker Red CMXRos staining

A 5-mm agar plug of *R. roseolus* was inoculated into 25 mL of 1/5MMN liquid medium and incubated at 25°C. The mycelia were then harvested, washed with sterile distilled water, and centrifuged at 4400 × g for 5 min. Approximately 100 mg of mycelia was transferred into microtube and treated with 1 mL of 10^{-8} M GR24 for 1 hour in dark. The control group was treated with sterile distilled water under the same conditions. After treatment, the mycelia were washed with sterile distilled water and centrifuged at 4400 × g for 5 min. The mycelia were subsequently stained with 100 nM MitoTracker Red CMXRos in medium containing 0.01% Tween 80 for 1 hour in dark. Mycelia were then washed with distilled water, centrifuged at 4400 × g for 5 min, and evenly spread onto glass slide. Observation using a fluorescence microscope was conducted for 10 biological replicates per experimental group, with 200 fluorescence images taken for each biological replicate. Fluorescence intensity was quantified using ImageJ and corrected for background noise. To reduce batch-to-batch variation, background-corrected fluorescence values were normalized within each batch using the formula below:

$$Fnorm\ (\%) = \frac{Fi - Fmin}{Fmax - Fmin}\ x\ 100\%$$

Fnorm = normalized fluorescence intensity (%)

Fi = background-corrected fluorescence intensity of each image

Fmax = highest background-corrected fluorescence intensity within the batch

Fmin = lowest background-corrected fluorescence intensity within the batch

Nitroblue tetrazolium (NBT) staining

A 5-mm agar plug of *R. roseolus* and *S. granulatus* were inoculated on glass slides coated with a thin layer of 1/5MMN agar and placed on 2% water agar in Petri dishes. The cultures were incubated in the dark at 25°C until the colonies reached approximately 1 cm in diameter. The incubation period was varied across isolates depend on their growth rates. Following incubation, colonies were treated for 1 h with 1 mL of GR24 or rac-GR24 at concentration 10^{-6} M, 10^{-8} M, or 10^{-10} M and later washed with 0.1 M PBS. For superoxide detection, each colony was flooded with 1 mL of 0.05% NBT solution for 1 h in the dark and washed with 0.1 M PBS. Superoxide accumulation was observed using blue formazan formed in NBT staining as an indicator. Each experimental group consisted of nine colonies as biological

repeats, with 200 hyphal tips examined per colony. Superoxide accumulation was calculated as the percentage of hyphal tips showing blue formazan relative to total number of hyphal tips examined.

To investigate the involvement of mitochondria and Ca^{2+} signaling in GR24 response of *R. roseolus*, several inhibitors and chelators were applied as pretreatments for 1 h prior to GR24 treatment and NBT staining. The synthesis of mitochondrial protein was inhibited using 1 mg/mL chloramphenicol (Besserer et al. 2009). Divalent ion such as Ca^{2+}, Mg^{2+}, Zn^{2+}, Mn^{2+}, Fe^{2+}, and Cu^{2+} was chelated using 0.5 mM EDTA (Richie et al. 2007; Zhai et al. 2022). Extracellular Ca^{2+} was chelated using 1 mM EGTA (Zhang et al. 2019; Dai et al. 2023). The activity of calcium channel was blocked using 10 μM verapamil(Latha and Mohan 2011). The concentration of inhibitor and chelator used in this experiment was based on previous studies in fungi and confirmed to not affecting basal superoxide accumulation of *R. roseolus*.

Primer design for RT-qPCR

Target genes were selected based on their relevance to the observed responses in our study and evidence from previous studies. Protein sequences of the corresponding genes from *Rhizopogon* (taxid:5375) and *Suillus* (taxid:5379) species were retrieved from NCBI and used as references. These protein sequences were searched against the *R. roseolus* genome available in our laboratory using local TBLASTN. Candidate genomic regions containing our target gene were extracted and analyzed using GENETYX software.

RT-qPCR primers were manually designed within conserved intron of the target genes. Primer properties were evaluated using OligoAnalyzer™. Primers were selected according to the following criteria: 18–25 nucleotides in length, an expected amplicon size of 70–200 bp, GC content of 40–60%, and a melting temperature (Tm) of 58–62°C, with a Tm difference of < 3°C between the forward and reverse primers. Primers terminating with G or C at the 3’ end were preferred. Primers with high potential of secondary structures or dimer ($\Delta G \leq -9$ kcal mol^{-1}) were avoided. Selected primer pair sequences are provided in Table S1. Primer specificity was confirmed by amplification of a single product of the expected size and by the presence of a single peak in melting-curve analysis (Fig. S1–S2).

Gene expression analysis with RT-qPCR

Ten 5-mm plugs agar of *R. roseolus* were inoculated into 25 mL 1/5MMN liquid medium and incubated in the dark at 25°C for ten days. After incubation, the mycelia were harvested aseptically and separated from the agar plugs. The harvested mycelia were washed with sterile distilled water and centrifuged at 4400 × g for 5 min to remove residual growth medium. Approximately 100 mg of mycelia was transferred into 1.5 μL microtube and treated with 1 mL of 10^{-8} M GR24 for 1 h. Control samples were treated with 1 mL sterile distilled water. Three independent biological replicates prepared for each treatment. Following treatment, the mycelia were centrifuge at 4400 × g for 5 min and immediately frozen in liquid nitrogen. Freeze-dried mycelia were finely ground using a pre-chilled mortar and pestle with addition of frequent

liquid nitrogen to the sample frozen until the mycelia formed a fine white powder. The mycelial powder was collected into prechilled microtubes using prechilled spatula.

Total RNA was extracted using TRIzol™ Reagent according to the instructions from manufacturer. The integrity and purity of extracted RNA were assessed by agarose gel electrophoresis and NanoDrop spectrophotometry, respectively. RNA samples with intact rRNA bands were kept at -80°C until subsequent analysis. The cDNA synthesis was conducted following the manufacturer protocol from ReverTra Ace® qPCR RT Master Mix with gDNA Remover (TOYOBO, Japan) in a T100 Thermal Cycler (Bio-Rad, USA). Quantitative PCR was performed according to the manufacturer protocol KOD SYBR™ qPCR/RT (TOYOBO, Japan) using a CFX Connect Real-Time System PCR (Bio-Rad, USA). During each RT-qPCR running, three biological replicates were analyzed for control and treatment group, with two or three technical replicates for each sample. Actin was used as the reference gene and analyzed in the same run as the target genes to minimize inter-run variation. The Cq value of target gene in each sample was normalized to Cq value of the reference gene (actin). Relative transcript abundance was calculated using the $2^{-\Delta\Delta Cq}$ method.

Statistical analysis

Experimental data recorded and managed using Microsoft Excel 2013. Statistical analyses and data visualization were performed using GraphPad Prism 10. Comparisons between two treatment groups were carried out using an independent t-test, while comparisons among multiple treatment groups were carried out using one-way analysis of variance (ANOVA), followed by Tukey's post hoc test for significantly different data ($P < 0.05$).

Results

Effects of GR24 on the growth and branching of ECM fungi

An initial screening was conducted using six ECM fungal isolates to evaluate the effect of GR24 on fungal growth and hyphal branching. Supplementation with 10^{-8} M GR24 for 5 weeks tended to increase mycelial dry weight in most ECM fungi isolates examined, with a statistically significant increase observed in *R. roseolus* ($P = 0.001987$) (Fig. 1). Furthermore, the effect of GR24 on hyphal branching was examined by direct treatment using a slide agar method. In the present of 10^{-8} M GR24, only *R. roseolus* showed a significant increase of number of primary hyphal branches ($P < 0.0001$) (Fig. 2). At a higher concentration of GR24 (10^{-6} M), significant increase in the number of primary hyphal branch was shown by *R. roseolus*, *S. granulatus*, *L. bicolor* ($P < 0.0001$). The branching response of *R. roseolus* was further examined with rac-GR24 at 10^{-8} M to evaluate stereochemistry effect. Between the tested compound, rac-GR24 induced the greatest increase in primary branch number, with an approximately 70% increase compared to the control (Fig. 3). At the same concentration, GR24 increased primary hyphal branching

by approximately 50%. Overall, these results suggest that GR24 differentially affects growth and branching among ECM fungal species depending on its stereochemistry and concentration.

Effects of GR24 on mitochondrial activity in ECM fungi

Based on previous result, the growth of *R. roseolus* was significantly affected by 10^{-8} M GR24, whereas no significant response was detected in *S. granulatus* with the same treatment. Using these two species, we examine whether the contrasting growth responses were associated with difference in mitochondrial activity. Fungal mycelia were exposed to 10^{-8} M GR24 for 1 hour and later stained with MitoTracker Red CMXRos, a mitochondrial probe which accumulation depend on mitochondrial membrane potential. The treatment significantly increased MitoTracker Red fluorescence intensity in *R. roseolus* by approximately 44% (P = < 0.000001) (Fig. 4A). In contrast, no significant change was observed in *S. granulatus* (Fig. 4B). Taken together, these results suggest an association between the GR24-induced growth and enhanced mitochondrial activity in *R. roseolus*.

Effects of GR24 on superoxide accumulation in ECM fungi

GR24 enhanced mitochondrial activity of *R. roseolus* as shown in Fig. 4A. We examined whether GR24 treatment also affects superoxide accumulation in ECM fungi because mitochondria are considered to be an important source of cellular superoxide. Colonies of *R. roseolus* and *S. granulatus* were exposed to each concentration and stereoisomer of GR24 for 1 hour, followed by NBT staining for 1 hour. In *R. roseolus*, both GR24 and rac-GR24 significantly increased superoxide accumulation in concentration-dependent manner, with greater accumulation observed at higher concentrations (Fig. 5A). In contrast, in *S. granulatus*, only higher concentrations of rac-GR24 significantly increased superoxide accumulation (Fig. 5B). Notably, *S. granulatus* showed no superoxide response at 10^{-8} M GR24, aligned with the lack of mitochondrial and growth responses at this concentration. Notably, superoxide accumulation was observed in actively growing hyphal tips and newly emerging branches (Fig. 5C–F). To further confirm whether GR24-induced superoxide accumulation was associated with mitochondrial activity, *R. roseolus* colonies were pretreated with chloramphenicol, a selective inhibitor of mitochondrial protein synthesis. The result in Fig. 6A shows that pretreatment with 1 mg/mL chloramphenicol for 1 hour significantly decreased significantly GR24-induced superoxide accumulation in *R. roseolus*. This result suggested mitochondria involvement in the superoxide accumulation triggered by GR24.

Effects of Ca^{2+} influx inhibitors on GR24-induced superoxide accumulation in R. roseolus

Previous studies reported that GR24 triggers a rapid and transient increase in intracellular free Ca^{2+} concentration in the AMF *G. margarita* (Moscatiello et al. 2014; Salvioli et al. 2016). However, it remains unclear whether the increase in intracellular Ca^{2+} concentration is driven by extracellular Ca^{2+} influx or mobilization of intracellular Ca^{2+} stores. To investigate Ca^{2+} involvement and source in the response of *R. roseolus* to GR24, we examined the effects of pretreatment with several Ca^{2+} modulators on GR24-induced superoxide accumulation. Pretreatment with the divalent cation chelator EDTA (0.5 mM) or the

Ca^{2+} chelator EGTA (1 mM) completely abolished GR24-induced peroxide accumulation (Fig. 6B). Pretreatment with the Ca^{2+}-channel blocker verapamil (10 µM) also eliminated the GR24-induced peroxide accumulation (Fig. 6B). These results support the idea that Ca^{2+} influx is required for GR24-induced superoxide accumulation.

Effects of GR24 on gene expression of R. roseolus

To determine whether GR24-induced morphological and cellular response in *R. roseolus* were associated with transcriptional changes, the expression of several relevant genes was examined using RT-qPCR. Treatment with 10^{-8} M GR24 for 1 h significantly increased expression of the cell-wall biosynthesis genes encoding chitin synthase by approximately 5.85-fold (P = 0.0044; Fig. 7A) and β-1,3-glucan synthase by approximately 2.78-fold (P = 0.0139; Fig. 7B). These transcriptional changes were consistent with the enhanced growth and hyphal branching after GR24 treatment.

Increase in mitochondrial membrane potential and superoxide accumulation that triggered by GR24 was also accompanied by transcriptional changes. GR24 increased expression of the mitochondrial respiration gene encoding cytochrome c oxidase by approximately 3.12-fold (P = 0.038; Fig. 7C), whereas ATP synthase was not significantly affected (Fig. 7D). GR24 also increased expression of gene encoding antioxidant Mn/Fe superoxide dismutase, approximately 6.35-fold (P = 0.0139; Fig. 7E). However, the same treatment did not significantly affect the expression of another antioxidant gene encoding thioredoxin reductase (Fig. 7F).

Expression of gene encoding calmodulin, a key Ca^{2+} sensor protein, was also observed using RT-qPCR. Treatment with 10^{-8} M GR24 for 1 hour increased calmodulin expression by approximately 3.84-fold compared with the control (P = 0.0169; Fig. 7G). Together with the inhibitory effect of Ca^{2+} modulators on GR24-induced superoxide accumulation, this gene expression further supports the involvement of Ca^{2+} signaling in the response of *R. roseolus* to GR24.

Discussion

SL responses have been reported in various plant-associated fungi, including arbuscular mycorrhizal, endophytic, and pathogenic fungi. In contrast, the role of SL in ectomycorrhizal (ECM) fungi remains largely unexplored. In this study, we found that SL analog GR24 differentially affects the growth and branching of ECM fungal species depending on its stereochemistry and concentration. These responses are consistent with previous studies in other fungi (Akiyama et al. 2010; Belmondo et al. 2017; Taulera et al. 2020; Fiorilli et al. 2022). Exposure to GR24 also triggers upregulation of cell-wall biosynthesis genes in ECM fungus *R. roseolus*. The effect of GR24 on genes encoding cell-wall remodelling proteins have also been reported in *Rhizophagus irregularis* and *Armillaria gallica* (Malbreil 2015; Liu et al. 2025).

Hyphal branching has been widely used as an indicator to screen fungal responsiveness to SL. However, hyphal branching does not always reflect symbiotic activity. Modified GR24 inhibited hyphal branching

while still able to stimulate germ-tube elongation and root colonization of AM fungus *R. irregularis* (Taulera et al. 2020). Beyond its effect on fungal growth and branching, SL also induced AM fungi to release symbiotic signal that are required for root colonization (Genre et al. 2013; Tsuzuki et al. 2016). In ECM fungus *P. tinctorius*, natural SL 5-deoxystrigol induced melanin secretion without affecting fungal growth (Herrera-Martínez et al. 2014). The absence of an obvious growth response does not necessarily exclude a role for SL in ECM symbiosis (Garcia et al. 2015). Therefore, focusing on hyphal branching as a response indicator may underestimate SL effect and overlook responsive fungi.

Beside hyphal growth and branching, GR24 effect in fungi is linked to mitochondrial activity. In AMF fungus *Gigaspora rosea*, GR24 rapidly enhanced mitochondrial metabolism and biogenesis to produce more energy (Besserer et al. 2006, 2008). Inhibition of these processes reduced the hyphal branching response to GR24 in *G. rosea* (Besserer et al. 2009). Consistent with these, the GR24-induced growth response in *R. roseolus* was accompanied by increased of mitochondrial membrane potential and expression of respiratory enzyme COX. Beside energy production, previous study in *B. cinerea* showed that mitochondrial response to GR24 also link to mitochondrial redox regulation including ROS homeostasis (Belmondo et al. 2017).

GR24 increased the accumulation of mitochondria-associated superoxide in *R. roseolus*. Superoxide, a primary ROS that generated by electron leakage from mitochondrial respiratory chain, is converted into hydrogen peroxide (H_2O_2) by superoxide dismutase (SOD) (Yaakoub et al. 2022). Coherently, GR24 also increased the expression of Mn/Fe-SOD in *R. roseolus*. In eukaryotes, Mn/Fe-SOD family predominantly localized in mitochondrial matrix and contributes to the detoxification of superoxide generated during mitochondrial respiration (Frye et al. 2022; Li et al. 2025). GR24-induced SOD expression or activity has also been observed in several plant-associated fungi (Besserer et al. 2008; Vannini et al. 2016; Rozpądek et al. 2018; Vogel et al. 2023). Furthermore, GR24-induced H_2O_2 accumulation has been reported in endophytic fungi *Mucor* sp. and phytopathogenic fungi *Botrytis cinerea* (Rozpądek et al. 2018; Vogel et al. 2023).

GR24 also affected broader antioxidant systems in fungi. In *G. margarita* and *A. gallica*, GR24 induced the activity of peroxide detoxifying enzyme such as catalase, peroxidase, and peroxiredoxin (Vannini et al. 2016; Hua et al. 2024). GR24 also induced the activity of glutathione-associated antioxidant such as glutathione-S-transferase and glutathione reductase in both fungi (Vannini et al. 2016; Hua et al. 2024). The thioredoxin system may also have role in GR24 response as mutation in thioredoxin reductase disrupted redox homeostasis and reduced *B. cinerea* sensitivity to SL (Belmondo et al. 2017). Together with our findings, these studies suggest that SL commonly trigger redox response involving ROS accumulation and antioxidant activity across various fungi. Therefore, we suggest that a simple ROS-based assays such as NBT staining may provide a useful preliminary screen for fungal responsiveness to SL.

Beside redox-related response, GR24 also induced a rapid and transient increase of cytosolic Ca^{2+} in the AM fungus *G. margarita* (Moscatiello et al. 2014; Salvioli et al. 2016). However, the source of this Ca^{2+}

increase remains unclear. Our results suggest that extracellular Ca^{2+} influx contributes to the GR24 response in *R. roseolus*, as blocking Ca^{2+} influx eliminating GR24-induced superoxide accumulation. An association between Ca^{2+} influx and ROS accumulation has also been reported in the filamentous fungus *Aspergillus fumigatus* and *Penicillium brevicompactum* (Chen et al. 2022; Ye et al. 2022). GR24 also enhanced expression of the gene encoding calmodulin in *R. roseolus*, providing further support for Ca^{2+} signaling involvement. Increased of cytosolic Ca^{2+} concentration that accompanied by upregulation of calmodulin encoding gene has been reported in *A. fumigatus* and *Cryptococcus neoformans* (Juvvadi et al. 2015; Cao et al. 2019).

Conclusions

The SL analog GR24 differentially affected the growth and branching of ECM fungal species depending on stereochemistry and concentration. Deeper investigation on *R. roseolus* TUFC10010 suggested that GR24 enhances mitochondrial activity and increases mitochondria-associated superoxide accumulation. The response of *R. roseolus* to GR24 required extracellular calcium influx. Coherently, GR24 upregulated genes involved in cell-wall biosynthesis, mitochondria respiratory chain, superoxide detoxification, and calcium signaling. Together, these findings provide novel mechanistic insight into SL responsiveness in ECM fungi by integrating morphological, cellular, and transcriptional analyses.

Declarations

Competing interests The authors declare no competing interests.

M.N.P conducted laboratory experiments, performed data analyses, and drafted the manuscript. K.N and S.C provided technical guidance on molecular methods. H.A. provided scientific guidance and research advice. T.A provided guidance on molecular methods and contributed to data interpretation. N.S provided scientific guidance on experimental protocols, contributed to data interpretation, and critically revised the manuscript. All authors read and approved the final version of the manuscript.

References

1. Akiyama K, Matsuzaki KI, Hayashi H (2005) Plant sesquiterpenes induce hyphal branching in arbuscular mycorrhizal fungi. Nature 435:824–827. https://doi.org/10.1038/nature03608
2. Akiyama K, Ogasawara S, Ito S, Hayashi H (2010) Structural requirements of strigolactones for hyphal branching in AM fungi. Plant Cell Physiol 51:1104–1117. https://doi.org/10.1093/pcp/pcq058
3. Alder A, Jamil M, Marzorati M et al (2012) The path from β-carotene to carlactone, a strigolactone-like plant hormone. Science (1979) 335:1348–1351. https://doi.org/10.1126/science.1215933
4. Belmondo S, Marschall R, Tudzynski P et al (2017) Identification of genes involved in fungal responses to strigolactones using mutants from fungal pathogens. Curr Genet 63:201–213.

https://doi.org/10.1007/s00294-016-0626-y

5. Besserer A, Bécard G, Jauneau A et al (2008) GR24, a synthetic analog of strigolactones, stimulates the mitosis and growth of the arbuscular mycorrhizal fungus Gigaspora rosea by boosting its energy metabolism. Plant Physiol 148:402–413. https://doi.org/10.1104/pp.108.121400
6. Besserer A, Bécard G, Roux C, Séjalon-Delmas N (2009) Role of mitochondria in the response of arbuscular mycorrhizal fungi to strigolactones. Plant Signal Behav 4:75–77. https://doi.org/10.4161/psb.4.1.7419
7. Besserer A, Puech-Pagès V, Kiefer P et al (2006) Strigolactones stimulate arbuscular mycorrhizal fungi by activating mitochondria. PLoS Biol 4:e226. https://doi.org/10.1371/journal.pbio.0040226
8. Cao C, Wang Y, Husain S et al (2019) A mechanosensitive channel governs lipid flippase-mediated echinocandin resistance in *Cryptococcus neoformans*. mBio 10. https://doi.org/10.1128/mBio.01952-19
9. Chen M, Wang J, Lin L et al (2022) Synergistic regulation of metabolism by Ca^{2+}/reactive oxygen species in *Penicillium brevicompactum* improves production of mycophenolic acid and investigation of the Ca^{2+} channel. ACS Synth Biol 11:273–285. https://doi.org/10.1021/acssynbio.1c00413
10. Cook CE, Whichard LP, Turner B et al (1966) Germination of witchweed (*Striga lutea* Lour.): Isolation and properties of a potent stimulant. Science (1979) 154:1189–1190. https://doi.org/10.1126/science.154.3753.1189
11. Dai M, Du W, Lu L, Zhang S (2023) Transcription factors SltA and CrzA reversely regulate calcium homeostasis under calcium-limited conditions. Appl Environ Microbiol 89. https://doi.org/10.1128/aem.01170-23
12. Decker EL, Alder A, Hunn S et al (2017) Strigolactone biosynthesis is evolutionarily conserved, regulated by phosphate starvation and contributes to resistance against phytopathogenic fungi in a moss, Physcomitrella patens. New Phytol 216:455–468. https://doi.org/10.1111/nph.14506
13. Dor E, Joel DM, Kapulnik Y et al (2011) The synthetic strigolactone GR24 influences the growth pattern of phytopathogenic fungi. Planta 234:419–427. https://doi.org/10.1007/s00425-011-1452-6
14. Fiorilli V, Forgia M, de Saint Germain A et al (2022) A structural homologue of the plant receptor D14 mediates responses to strigolactones in the fungal phytopathogen *Cryphonectria parasitica*. New Phytol 234:1003–1017. https://doi.org/10.1111/nph.18013
15. Frye KA, Sendra KM, Waldron KJ, Kehl-Fie TE (2022) Old dogs, new tricks: New insights into the iron/manganese superoxide dismutase family. J Inorg Biochem 230. https://doi.org/10.1016/j.jinorgbio.2022.111748
16. Fujita M, Tanaka T, Kusajima M et al (2024) Enhanced disease resistance against *Botrytis cinerea* by strigolactone-mediated immune priming in *Arabidopsis thaliana*. J Pestic Sci 49:186–194. https://doi.org/10.1584/JPESTICS.D24-019
17. Garcia K, Delaux PM, Cope KR, Ané JM (2015) Molecular signals required for the establishment and maintenance of ectomycorrhizal symbioses. New Phytol 208:79–87. https://doi.org/10.1111/nph.13423

18. Genre A, Chabaud M, Balzergue C et al (2013) Short-chain chitin oligomers from arbuscular mycorrhizal fungi trigger nuclear Ca^{2+} spiking in *Medicago truncatula* roots and their production is enhanced by strigolactone. New Phytol 198:190–202. https://doi.org/10.1111/nph.12146
19. Gomez-Roldan V, Fermas S, Brewer PB et al (2008) Strigolactone inhibition of shoot branching. Nature 455:189–194. https://doi.org/10.1038/nature07271
20. Hamiaux C, Drummond RSM, Janssen BJ et al (2012) DAD2 is an α/β hydrolase likely to be involved in the perception of the plant branching hormone, strigolactone. Curr Biol 22:2032–2036. https://doi.org/10.1016/j.cub.2012.08.007
21. Herrera-Martínez A, Ruiz-Medrano R, Galván-Gordillo SV et al (2014) A 2-component system is involved in the early stages of the *Pisolithus tinctorius-Pinus greggii* symbiosis. Plant Signal Behav 9:e28604. https://doi.org/10.4161/psb.28604
22. Hua Z, Teng X, Huang J et al (2024) The *Armillaria* response to *Gastrodia elata* is partially mediated by strigolactone-induced changes in reactive oxygen species. Microbiol Res 278. https://doi.org/10.1016/j.micres.2023.127536
23. Juvvadi PR, Muñoz A, Lamoth F et al (2015) Calcium-mediated induction of paradoxical growth following caspofungin treatment is associated with calcineurin activation and phosphorylation in *Aspergillus fumigatus*. Antimicrob Agents Chemother 59:4946–4955. https://doi.org/10.1128/AAC.00263-15
24. Latha JNL, Mohan PM (2011) Role of cell wall bound calcium in *Neurospora crassa*. Microbiol Res 166:419–429. https://doi.org/10.1016/j.micres.2010.10.001
25. Li H, Sheng RC, Wang YH et al (2025) Mitochondrial complex member VdNuo1 recruits superoxide dismutases VdSOD2/4 to maintain superoxide anion homeostasis during pathogenesis in *Verticillium dahliae*. Mol Plant Pathol 26. https://doi.org/10.1111/mpp.70149
26. Liu L, Li B, Li S et al (2025) Transcriptomics reveals the mechanism of branching production in response to GR24 in *A. gallica* 541. Sci Rep 15. https://doi.org/10.1038/s41598-025-09015-w
27. Malbreil MRC (2015) *Rhizophagus irregularis* gene regulation in early steps of AMF-plant symbiosis. In: Accession: GSE67913. https://www.ncbi.nlm.nih.gov/geo/query/acc.cgi?acc=GSE67913. Accessed 30 Sep 2026
28. Moscatiello R, Sello S, Novero M et al (2014) The intracellular delivery of TAT-aequorin reveals calcium-mediated sensing of environmental and symbiotic signals by the arbuscular mycorrhizal fungus *Gigaspora margarita*. New Phytol 203:1012–1020. https://doi.org/10.1111/nph.12849
29. Nakamura H, Xue YL, Miyakawa T et al (2013) Molecular mechanism of strigolactone perception by DWARF14. Nat Commun 4. https://doi.org/10.1038/ncomms3613
30. Putra IP, Aimi T, Shimomura N (2022) Cytological comparison of mycelial aggregates of *Rhizopogon roseolus* with and without the ectomycorrhiza host. Mycologia 114:533–543. https://doi.org/10.1080/00275514.2022.2035156
31. Richie DL, Fuller KK, Fortwendel J et al (2007) Unexpected link between metal ion deficiency and autophagy in *Aspergillus fumigatus*. Eukaryot Cell 6:2437–2447. https://doi.org/10.1128/EC.00224-

07

32. Rozpądek P, Domka AM, Nosek M et al (2018) The role of strigolactone in the cross-talk between *Arabidopsis thaliana* and the endophytic fungus *Mucor* sp. Front Microbiol 9. https://doi.org/10.3389/fmicb.2018.00441
33. Salvioli A, Ghignone S, Novero M et al (2016) Symbiosis with an endobacterium increases the fitness of a mycorrhizal fungus, raising its bioenergetic potential. ISME J 10:130–144. https://doi.org/10.1038/ismej.2015.91
34. Shimomura N, Matsuda M, Ariyoshi K, Aimi T (2012) Development of mycelial slurries containing surfactant for cultivation of the edible ectomycorrhizal mushroom *Rhizopogon roseolus* (syn. Rhizopogon rubescens). Botany 90:839–844. https://doi.org/10.1139/b2012-054
35. Steinkellner S, Lendzemo V, Langer I et al (2007) Flavonoids and strigolactones in root exudates as signals in symbiotic and pathogenic plant-fungus interactions. Molecules 12:1290–1306. https://doi.org/10.3390/12071290
36. Taulera Q, Lauressergues D, Martin K et al (2020) Initiation of arbuscular mycorrhizal symbiosis involves a novel pathway independent from hyphal branching. Mycorrhiza 30:491–501. https://doi.org/10.1007/s00572-020-00965-9
37. Torres-Vera R, García JM, Pozo MJ, López-Ráez JA (2014) Do strigolactones contribute to plant defence? Mol Plant Pathol 15:211–216. https://doi.org/10.1111/mpp.12074
38. Tsuzuki S, Handa Y, Takeda N, Kawaguchi M (2016) Strigolactone-induced putative secreted protein 1 is required for the establishment of symbiosis by the arbuscular mycorrhizal fungus *Rhizophagus irregularis*. Mol Plant Microbe Interact 29:277–286. https://doi.org/10.1094/MPMI-10-15-0234-R
39. Umehara M, Hanada A, Yoshida S et al (2008) Inhibition of shoot branching by new terpenoid plant hormones. Nature 455:195–200. https://doi.org/10.1038/nature07272
40. Vannini C, Carpentieri A, Salvioli A et al (2016) An interdomain network: The endobacterium of a mycorrhizal fungus promotes antioxidative responses in both fungal and plant hosts. New Phytol 211:265–275. https://doi.org/10.1111/nph.13895
41. Vogel D, Hills P, Moore JP (2023) Strigolactones GR-24 and Nijmegen applications result in reduced susceptibility of tobacco and grapevine plantlets to *Botrytis cinerea* infection. Plants 12. https://doi.org/10.3390/plants12183202
42. Wang Y, Bouwmeester HJ (2018) Structural diversity in the strigolactones. J Exp Bot 69:2219–2230
43. Xie X (2016) Structural diversity of strigolactones and their distribution in the plant kingdom. J Pestic Sci 41:175–180. https://doi.org/10.1584/jpestics.J16-02
44. Yaakoub H, Mina S, Calenda A et al (2022) Oxidative stress response pathways in fungi. Cell Mol Life Sci 79
45. Ye J, Wang Y, Li X et al (2022) Synergistic antifungal effect of a combination of iron deficiency and calcium supplementation. Microbiol Spectr 10:1–18. https://doi.org/10.1128/spectrum.01121-22

46. Yoneyama K, Mori N, Sato T et al (2018) Conversion of carlactone to carlactonoic acid is a conserved function of MAX1 homologs in strigolactone biosynthesis. New Phytol 218:1522–1533. https://doi.org/10.1111/nph.15055
47. Zhai P, Ma Y, Xu H, Lu L (2022) Molecular Characterization and the Essential Biological Function of the Metal Chaperone Protein MtmA in Aspergillus fumigatus. Appl Environ Microbiol 88. https://doi.org/10.1128/aem.00182-22
48. Zhang W, Hu C, Hussain M et al (2019) Role of low-affinity calcium system member Fig. 1 homologous proteins in conidiation and trap-formation of nematode-trapping fungus *Arthrobotrys oligospora*. Sci Rep 9. https://doi.org/10.1038/s41598-019-40493-x

Figures

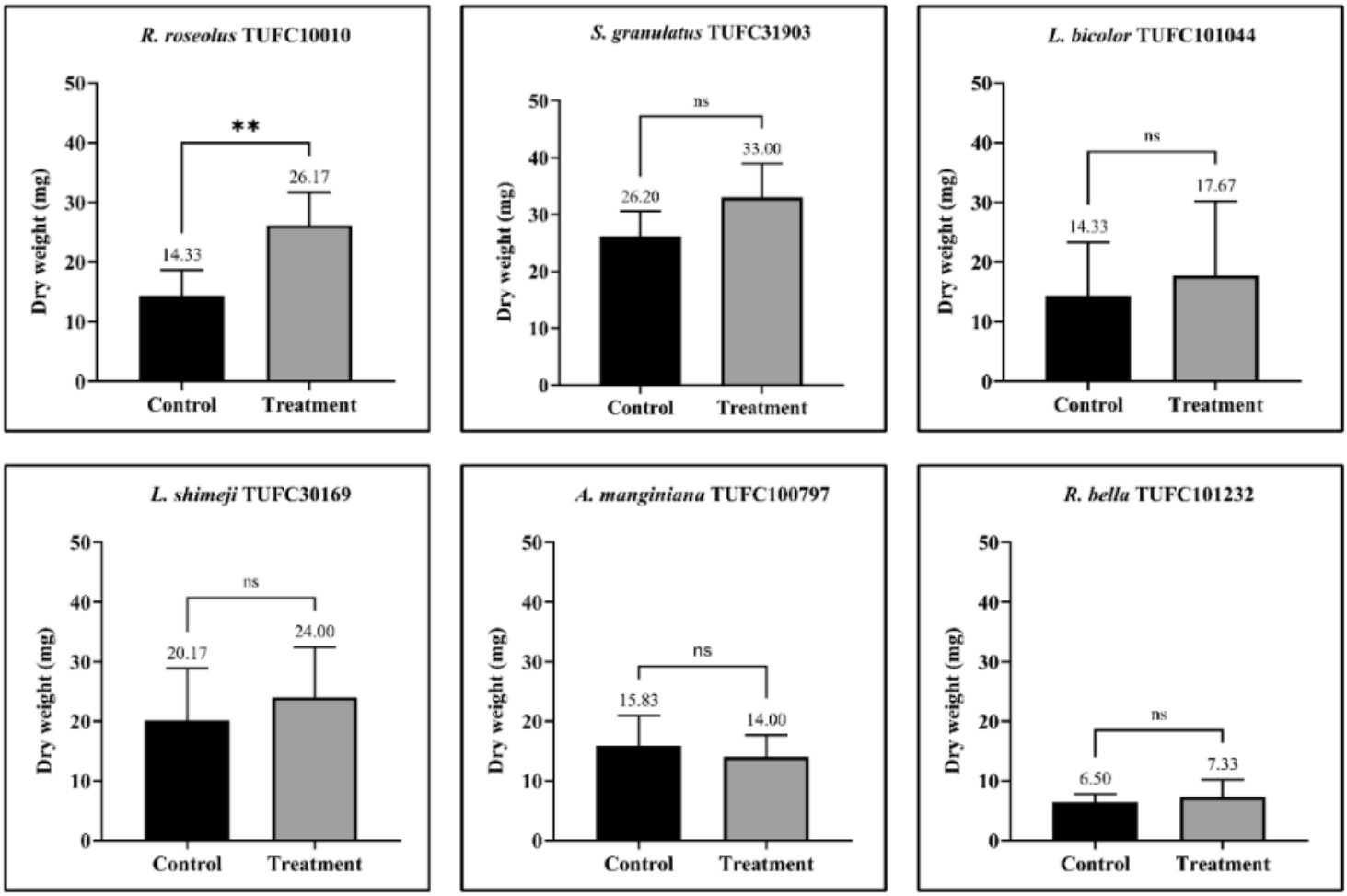


Figure 1

Effects of GR24 on the growth of ectomycorrhizal fungi. Dry weight was determined for several ectomycorrhizal fungal isolates grown for 5 weeks in 1/5MMN liquid medium supplemented with 10 nM (10^{-8} M) GR24. Data are presented as means ± SD (n = 4–6 biological replicates). Statistical analysis was conducted using independent t-tests; $P < 0.01$ (**), not significant (ns).

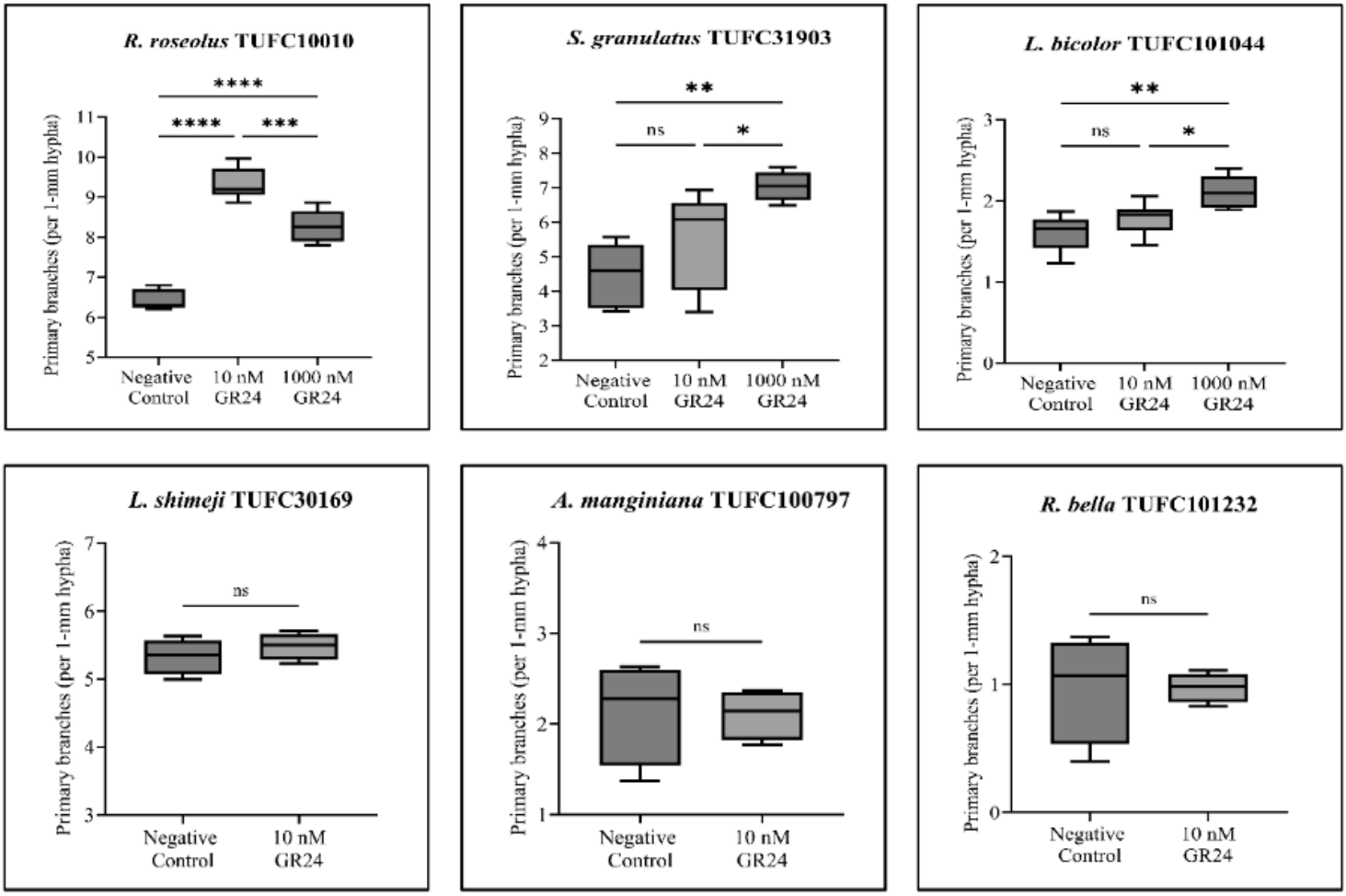


Figure 2

Effects of GR24 on hyphal branching of ectomycorrhizal fungi. The number of primary branches was quantified after treatment with 10 nM (10^{-8} M) or 1000 nM (10^{-6} M) GR24. Data were obtained from 4–5 biological replicates with primary branches were counted from 30 hyphae within 1000 µm from the hyphal tips.

Statistical analysis was conducted using independent t-tests; $P < 0.05$ (*), $P < 0.01$ (**), $P < 0.001$ (***), $P < 0.0001$ (****), not significant (ns).

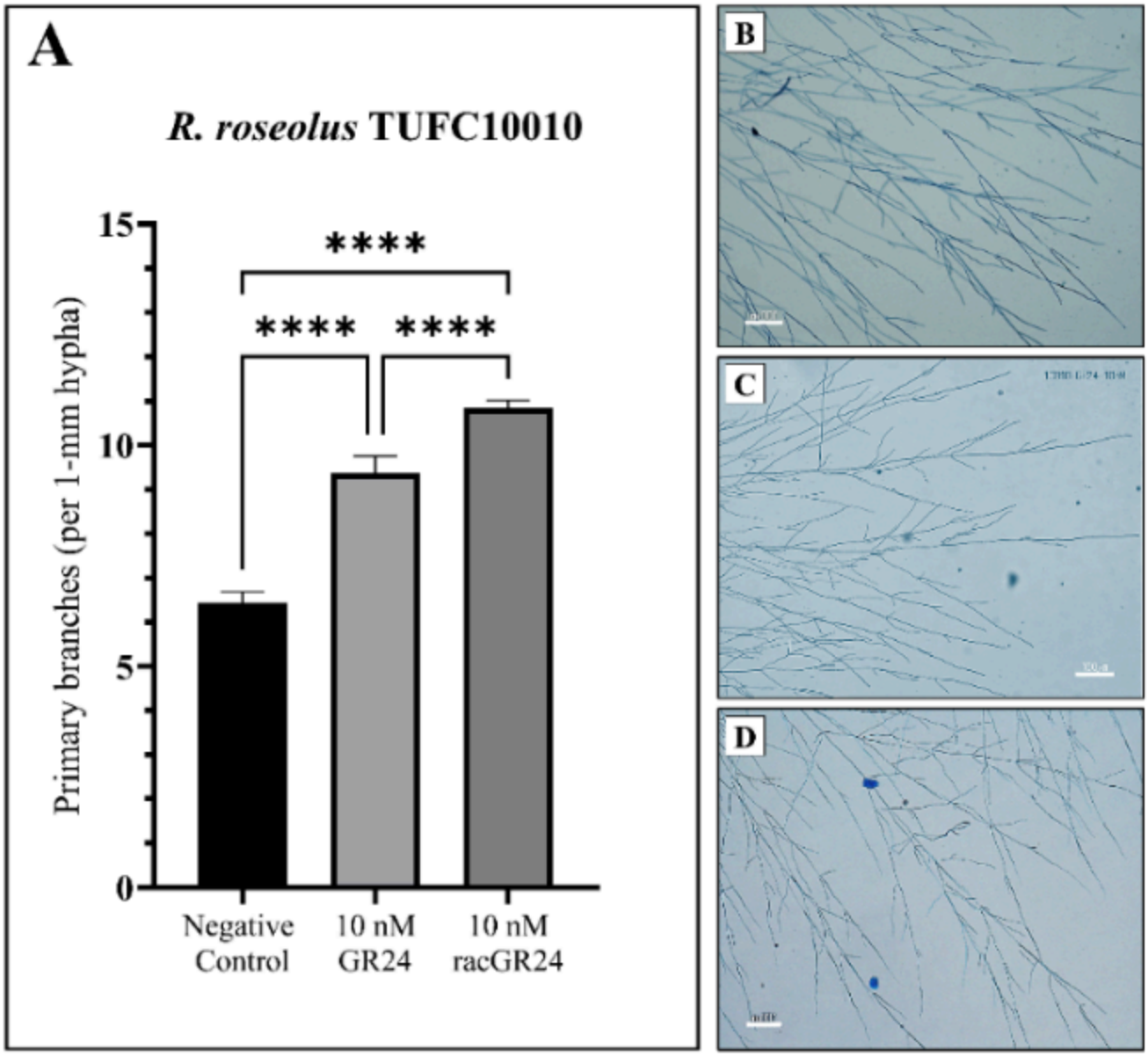


Figure 3

Effects of GR24 and rac-GR24 on hyphal branching of *Rhizopogon roseolus* TUFC10010. (A) Number of primary hyphal branches under treatment with 10 nM (10^{-8} M) GR24 or rac-GR24. Data are represented as means ± SD (n = 6–10 biological replicates). For each biological replicate, branches were counted from 30 hyphae within 1000 μm from the hyphal tips. Statistical significance was analyzed using one-way ANOVA followed by Tukey's post hoc test; $P < 0.0001$ (****). (B–D) Representative images of *R. roseolus* hyphae under control condition (B), GR24 treatment (C), and rac-GR24 treatment (D). Bar line = 100 μm.

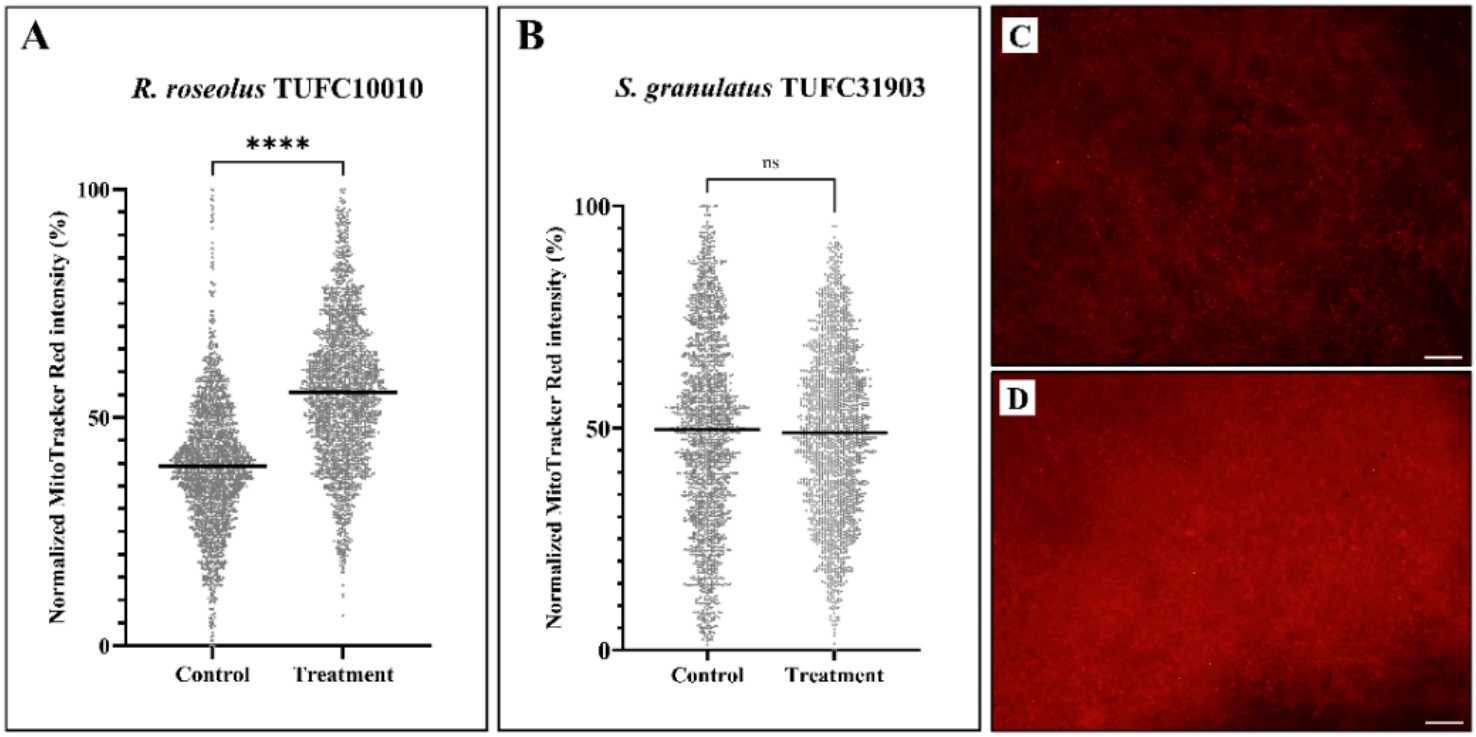


Figure 4

Effects of GR24 on mitochondrial activity in ectomycorrhizal fungi. Mitochondrial membrane potential was assessed using MitoTracker Red CMXRox after treatment with 10 nM (10^{-8} M) GR24 in (A) *Rhizopogon roseolus* TUFC10010 and (B) *Suillus granulatus* TUFC 31903. Representative images show *R. roseolus* TUFC10010 mycelia under (C) control condition and (D) treatment with 10 nM GR24. Data were obtained from 10 biological replicates, with 200 images captured evenly across the mycelial surface for each replicate. Statistical analysis was conducted using independent t-tests; $P < 0.0001$ (****), not significant (ns). Bar line = 100 µm.

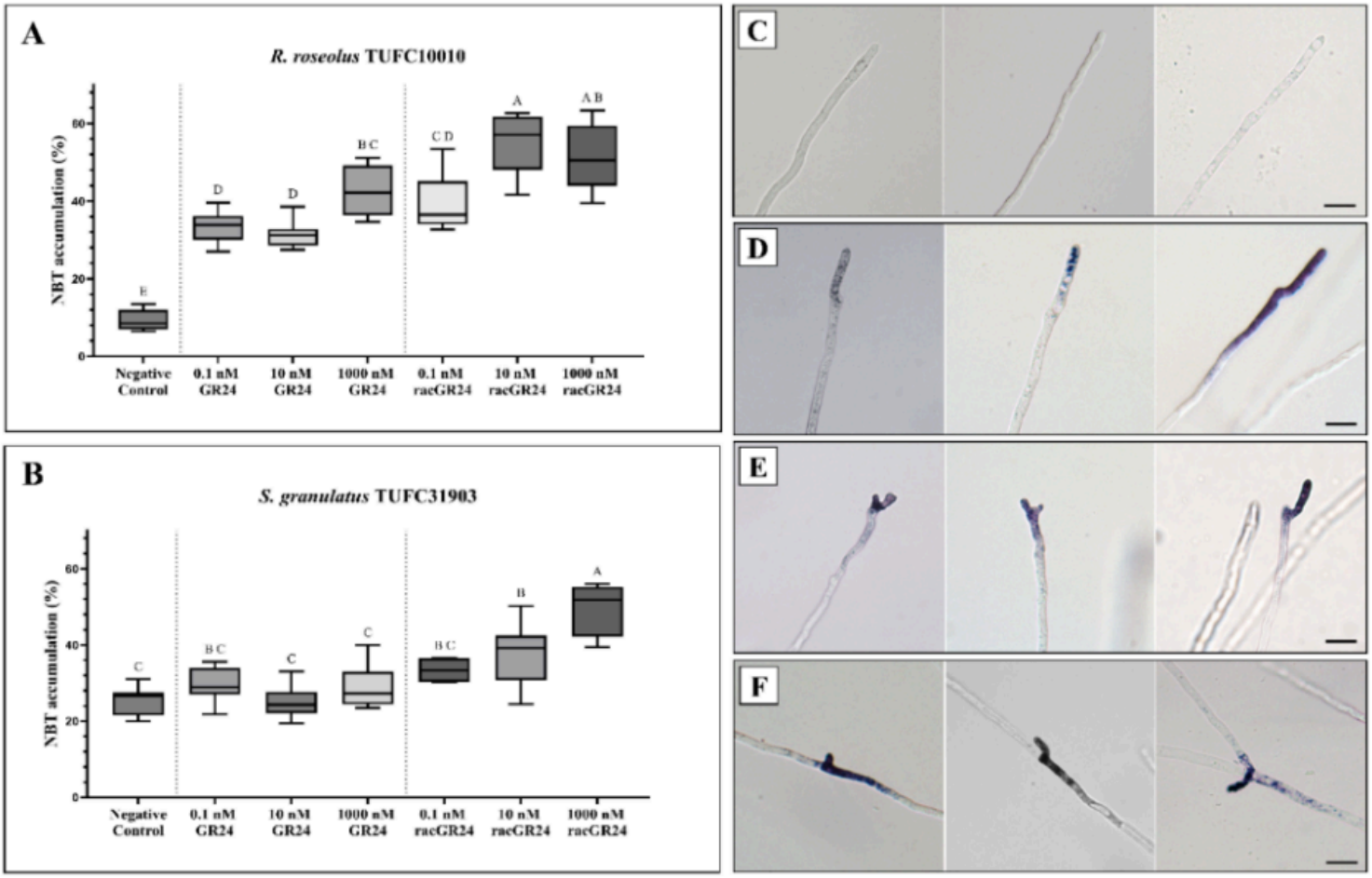


Figure 5

Effects of GR24 on superoxide accumulation in ectomycorrhizal fungi. Superoxide accumulation was assessed using nitroblue tetrazolium (NBT) after treatment with several concentration of GR24 or rac-GR24 for 1 hour in (A) *Rhizopogon roseolus* TUFC10010 and (B) *Suillus granulatus* TUFC 31903. Representative images of *R. roseolus* TUFC10010 show (C) hyphal tips without detectable superoxide accumulation and (D–F)actively growing hyphal tips and newly emerging branches with prominent superoxide accumulation. Data were obtained from 8–9 biological replicates, with 200 hyphal tips examined per replicate. Statistical significance was analyzed using one-way ANOVA followed by Tukey's post hoc test. Different letters indicate significant differences among groups ($P < 0.05$). Bar line = 10 μm.

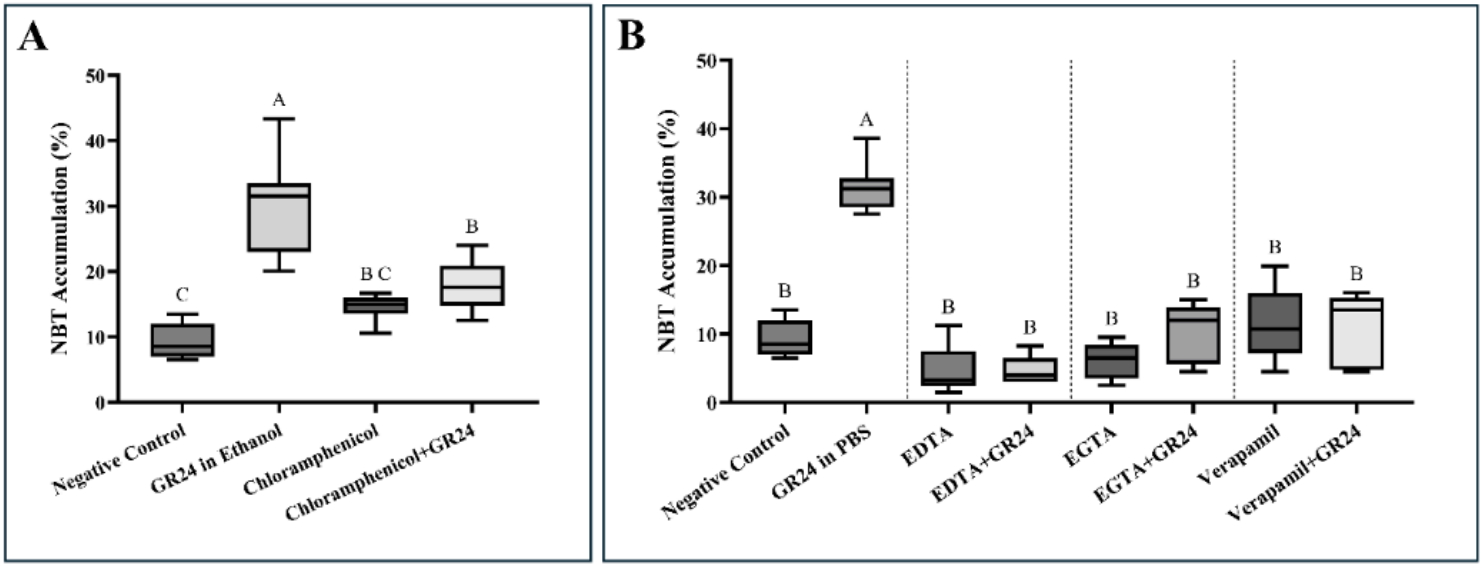


Figure 6

Effects of pharmacological inhibitors on GR24-induced superoxide accumulation in *Rhizopogon roseolus* TUFC10010. (A) 1 mg/mL chloramphenicol as inhibitor of mitochondrial protein synthesis, (B) Ca^{2+} influx inhibitors: 0.5 mM EDTA as extracellular divalent-ion chelator; 1 mM EGTA as extracellular Ca^{2+} chelator; and 10 μM verapamil as Ca^{2+} channel blocker. Data were obtained from 5–8 biological replicates, with 200 hyphal tips examined per replicate. Statistical significance was analyzed using one-way ANOVA followed by Tukey's post hoc test. Different letters indicate significant differences among groups ($P < 0.05$).

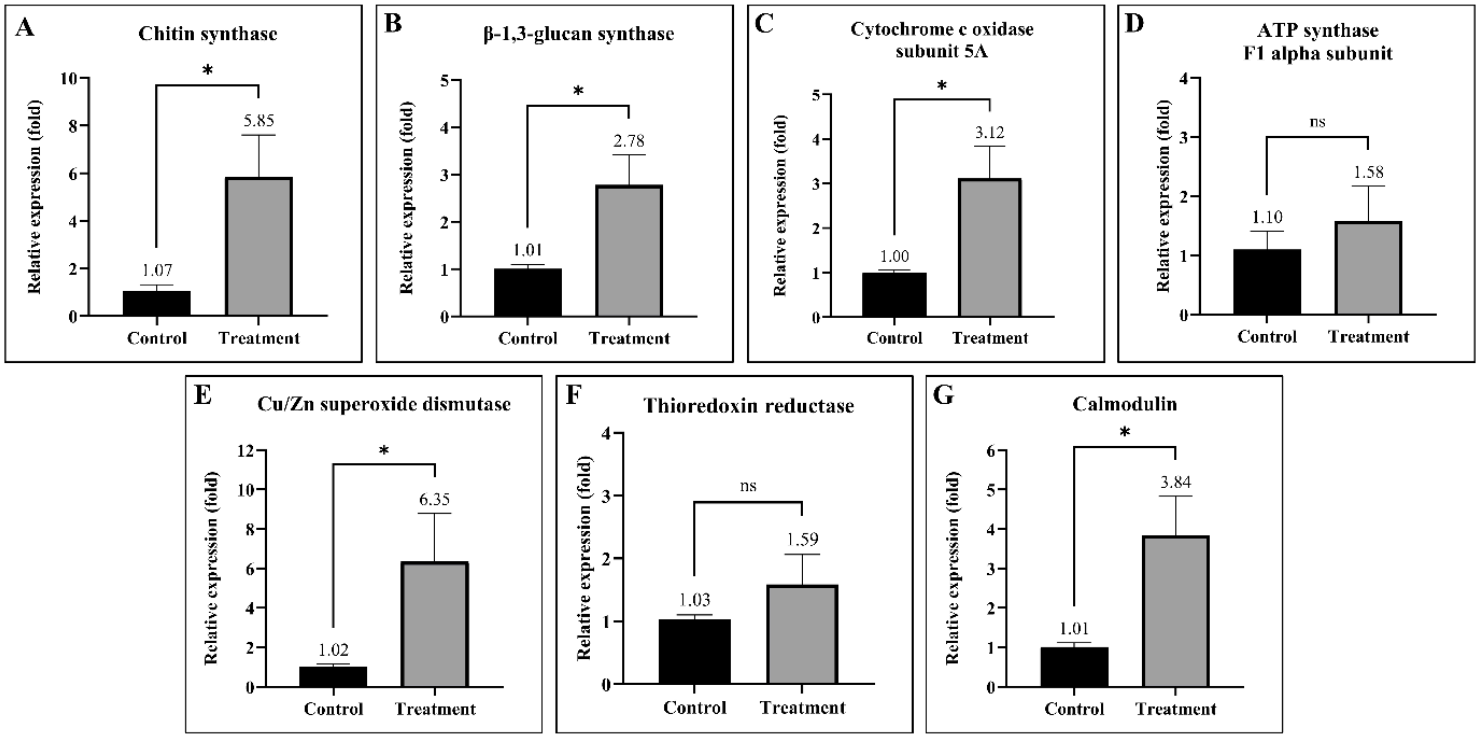


Figure 7

Effects of GR24 on gene expression of *Rhizopogon roseolus* TUFC10010. Gene expression was analyzed after treatment with 10 nM (10^{-8} M) GR24 for 1 hour. The analyzed genes were associated with (A–B) cell-wall biosynthesis, (C–D) mitochondrial respiration, (E–F) antioxidant activity, and (G) Ca^{2+} signaling. Relative gene expression was calculated using the $2^{-\Delta\Delta Cq}$ method (n=3), with actin as the reference gene. Statistical analysis was conducted using independent t-tests; $P < 0.05$ (*); not significant (ns).

Supplementary Files

This is a list of supplementary files associated with this preprint. Click to download.

- SupplementaryMaterial.docx